Self-Trapping of Exciton-Polariton Condensates in GaAs Microcavities

Dario Ballarini,[1] Igor Chestnov,[2,3,4] Davide Caputo,[1,5] Milena De Giorgi,[1] Lorenzo Dominici,[1] Kenneth West,[6] Loren N. Pfeiffer,[6] Giuseppe Gigli,[1,5] Alexey Kavokin,[2,3,7,8] and Daniele Sanvitto[1,9]

[1]*CNR NANOTEC—Institute of Nanotechnology, Via Monteroni, 73100 Lecce, Italy*
[2]*Westlake University, School of Science, 18 Shilongshan Road, Hangzhou 310024, Zhejiang Province, China*
[3]*Westlake Institute for Advanced Study, Institute of Natural Sciences, 18 Shilongshan Road, Hangzhou 310024, Zhejiang Province, China*
[4]*Vladimir State University, 600000 Vladimir, Russia*
[5]*University of Salento, Via Arnesano, 73100 Lecce, Italy*
[6]*PRISM, Princeton Institute for the Science and Technology of Materials, Princeton Unviversity, Princeton, New Jersey 08540, USA*
[7]*Spin Optics Laboratory, St. Petersburg State University, St. Petersburg 198504, Russia*
[8]*Russian Quantum Centre, 100 Novaya St., 143025 Skolkovo, Moscow Region, Russia*
[9]*INFN, Sezione di Lecce, 73100 Lecce, Italy*

(Received 19 October 2018; published 23 July 2019)

The self-trapping of exciton-polariton condensates is demonstrated and explained by the formation of a new polaronlike state. Above the polariton lasing threshold, local variation of the lattice temperature provides the mechanism for an attractive interaction between polaritons. Because of this attraction, the condensate collapses into a small bright spot. Its position and momentum variances approach the Heisenberg quantum limit. The self-trapping does not require either a resonant driving force or a presence of defects. The trapped state is stabilized by the phonon-assisted stimulated scattering of excitons into the polariton condensate. While the formation mechanism of the observed self-trapped state is similar to the Landau-Pekar polaron model, this state is populated by several thousands of quasiparticles, in a striking contrast to the conventional single-particle polaron state.

DOI: 10.1103/PhysRevLett.123.047401

Introduction.—Self-trapping is an intriguing physical effect that is rather rarely encountered in solid state systems. Among its most well-known manifestations are the phonon self-trapping of charge carriers leading to the polaron formation [1,2] and the magnetic self-trapping of carriers or excitons in diluted magnetic semiconductors leading to the magnetic polaron formation [3,4]. Both polaronic self-trapping mechanisms seem incompatible with the Bose-Einstein condensation as the latter leads to the formation of spatially extended coherent many-body states: the bosonic condensates. Nevertheless, experimentally, bosonic condensates of half-light-half-matter quasiparticles, exciton polaritons, formed in semiconductor microcavities [5] are frequently spatially localized [6]. The localization is due to the stationary disorder potential necessarily present in the microcavity plane [7], and/or due to finite size optical spots used to generate the polaritons [8]. The interplay and competition between magnetic self-trapping and Bose-Einstein condensation of exciton polaritons was analyzed theoretically [9]. In nonmagnetic systems the polariton liquid intrinsically tends to delocalize as the polaritons repel each other and are repelled by the reservoir of noncondensed excitons formed by a nonresonant optical pumping. It comes as a surprise, that in certain experimental conditions, condensates of polaritons collapse in real space leading to the formation of dense droplets [10].

In this Letter, we demonstrate that self-trapping is a general feature of polariton condensates due to the coupling with the exciton reservoir by reporting the extreme localization occurring at the condensation threshold under nonresonant excitation. We observe the unpinned polariton droplet whose area is 2 orders of magnitude smaller than the area of the excitation light spot. Looking at the blueshift of the condensate energy and the image of the condensate in the reciprocal space, we conclude on the origin of self-trapping. The shrinkage of the condensate wave function is induced by the local heating of the crystal lattice in the center of the pump-beam area. The tightly localized state of the condensate is stabilized by the nonlinearity caused by the condensate-reservoir coupling.

The observed state constitutes a new phase of a bosonic condensate that may be referred to as the bosonic polaron state. In contrast to a conventional (fermionic) polaron, this state is characterized by a local lattice temperature variation rather than by strain. In our system the polaron wave function represents the localized many-body wave function of a bosonic condensate. Self-trapping of exciton polaritons is a new phenomenon in the physics of bosonic condensates

with promising prospects for applications in polariton simulators [11,12]. A similar scenario, with the emergence of a heat-assisted, sink-type steady state, has been recently predicted in one-dimensional polariton wires [13].

Results.—The system under study is a high quality factor semiconductor microcavity characterized by a long polariton lifetime $\tau = 100$ ps and a strongly reduced density of defects [14]. Similar samples have been recently made available by the advanced control of the molecular beam epitaxy growth process, that allows for the observation of thermalized polariton condensation and for the efficient ballistic propagation of polaritons in the cavity plane [15–17]. The long polariton lifetime (10 times longer than most of previous works in the literature) and the high spatial homogeneity of the present sample are essential requirements to allow the occupation of the lowest energy state without accidental localization in local potential minima (defects). The microcavity is excited by a continuous wave laser, tuned ≈100 meV above the exciton resonance, and the photoluminescence (PL) is collected by imaging spectroscopy, allowing for two-dimensional (2D) energy-resolved detection of the emission in both the real space and the reciprocal space (see also Supplemental Material [18]).

In Figs. 1(a)–1(f), the energy-resolved PL both in momentum (left column) and real space (right column) is shown for increasing excitation powers (from top to bottom). Carrier relaxation leads to the formation of a large population of excitons (exciton reservoir) with in-plane wave vector k beyond the light cone. The exciton relaxation mediated by phonon scattering leads to the occupation of radiative polariton states at the bottom of the lower polariton branch (LPB), close to $k = 0$ [see Figs. 1(a) and 1(b)]. Polariton condensation occurs when the balance between gain (stimulated scattering into the bottom of the LPB) and losses (mainly radiative emission) is achieved, a condition that is fulfilled in Figs. 1(c) and 1(d). The emission of the polariton condensate appears blueshifted by ≈2 meV: this is due to the repulsive exciton-exciton interactions in the spatial region where the exciton reservoir is highly populated. The white dashed line in Figs. 1(b), 1(d), and 1(f) denotes the bottom energy of the LPB, that follows the intensity profile of the exciting laser given the short exciton diffusion length (< 3 μm). In Fig. 1(e), the two bright points at $k \approx \pm 2$ μm^{-1} correspond to polaritons propagating either inwards, bringing the polariton density to the center of the excitation spot, or outwards (in the tail regions) due to the repulsion from the reservoir [19,20]. In the same Fig. 1(e), the central emission with a wide k distribution around $k = 0$ corresponds to the spatially localized polariton condensate shown in Fig. 1(f).

Surprisingly, we found that, even well above the condensation threshold, the emission is localized in a small spatial region of less than a 5 μm^2 area. Note that the Gaussian laser spot excites a 10^2 larger area and the

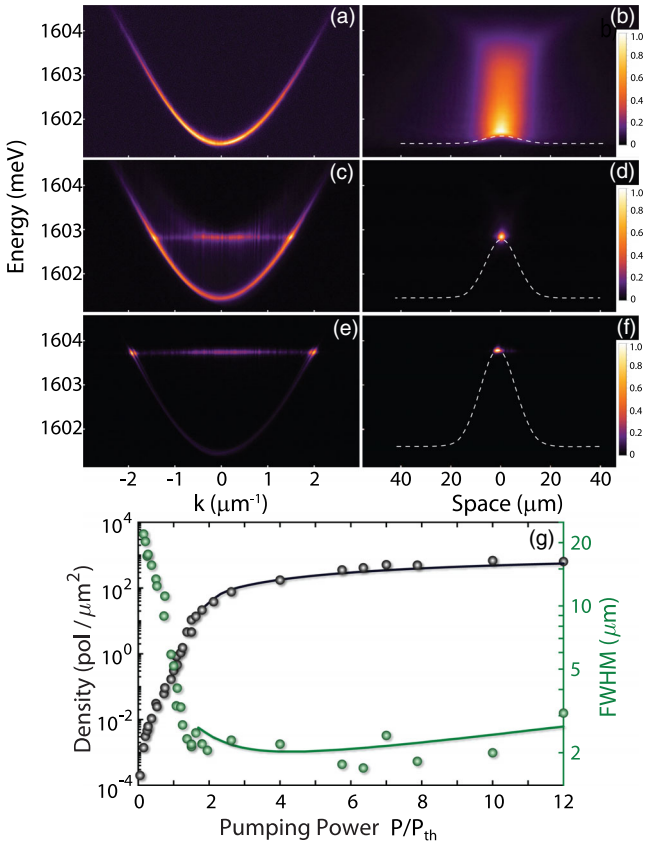

FIG. 1. (a)–(f) Energy-resolved (vertical axis) polariton emission in momentum (left column) and real space (right column) along the k_x and x directions, respectively. The wave vector k is proportional to the in-plane momentum, $k = p/\hbar = (2\pi/\lambda)\sin\theta$, with λ being the polariton wavelength and θ being the incidence angle. Pump power increases from $P = 0.42P_{\mathrm{th}}$, $P = P_{\mathrm{th}}$, and $P = 3.3P_{\mathrm{th}}$ from top to bottom rows. (g) Polariton density vs excitation power (black points) normalized at the threshold value (around $P_{\mathrm{th}} = 40$ mW). The FWHM (Gaussian fit) of the polariton distribution in space is shown (green points) to shrink from values comparable to that of the laser spot (FWHM=20 μm) at low density to less than 2 μm above P_{th}. Solid lines are the calculated density (black line) and spatial FWHM (green line) as obtained from numerical simulations (above threshold).

localization is observed also if changing the position of the excitation spot on the sample; i.e., it is independent of the microscopic details of the sample such as possible defects. The shrinking of the polariton emission above threshold is quantitatively described in Fig. 1(g), where the spatial full-width-half-maximum (FWHM) of the polariton emission is shown (green points) for increasing excitation powers and compared to the emission intensity (black points), proportional to the polariton density (see Supplemental Material [18]).

In Fig. 2, the emission of the polariton condensate is shown for different sizes of the excitation laser spot (FWHM = 20, 30, 40 μm). The pump power has been adjusted to have the same blueshift of the polariton

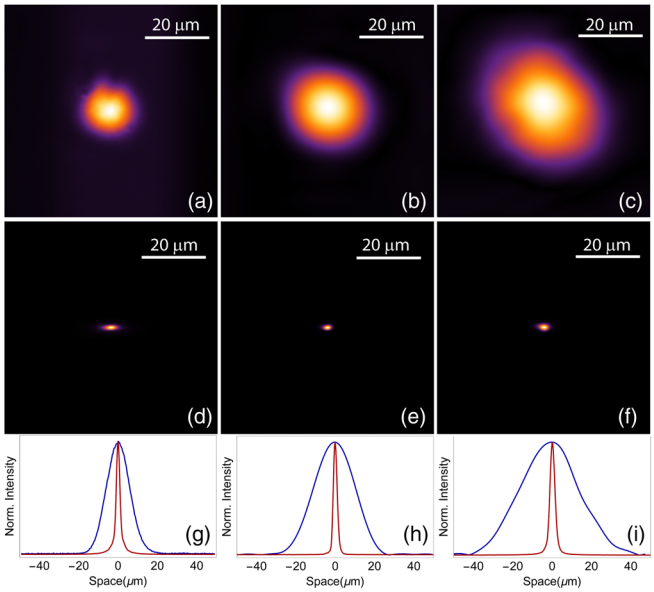

FIG. 2. (a)–(c) Three different sizes of the nonresonant pumping laser spot: FWHM is 20, 30 and 40 μm in (a), (b), and (c), respectively. (d)–(f) Condensate emission in real space corresponding to the excitation spots shown in (a), (b), and (c), respectively. The polaron condensate is always localized in a spot of less than 5 μm diameter. (g)–(i) The vertical cross section of the intensity profile of the pumping laser [blue line, corresponding to (a), (b) and (c), respectively] and of the condensate [red line, corresponding to (d), (e), and (f), respectively].

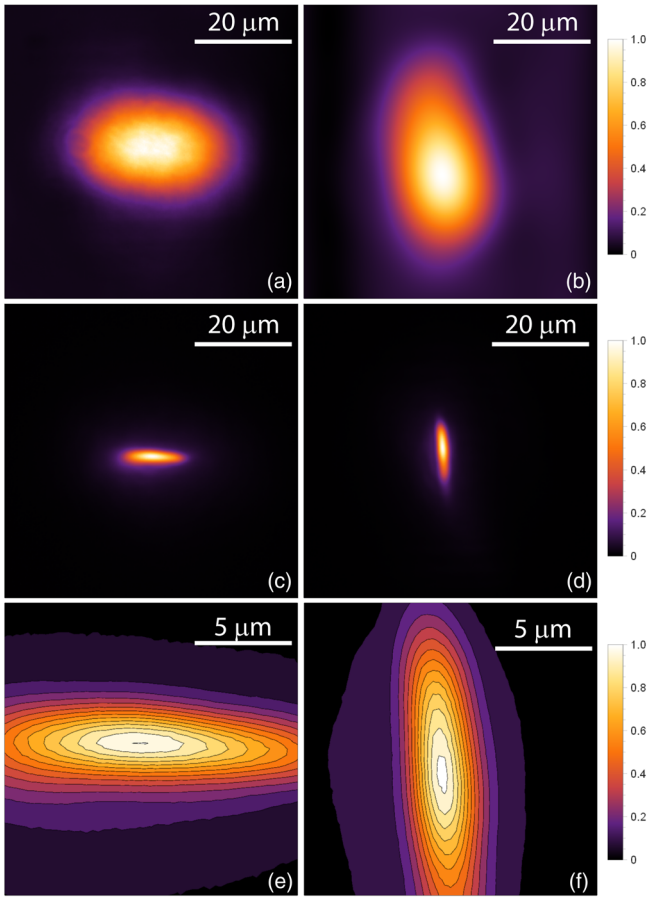

FIG. 3. (a),(b) Pumping spots of elliptical shapes with horizontal and vertical elongation, respectively. (c),(d) Condensate emission in real space corresponding to the excitation shown in (a) and (b), respectively. (e),(f) Contour plot of the condensate emission intensity [magnification of (c) and (d), respectively].

condensate in all cases despite of the different excitation areas. The full two-dimensional collapse of the polariton condensate is clearly evident by comparing the pump spot intensity (top row) with the PL intensity (second row), showing localized emission from a spatial region two orders of magnitude smaller than the excitation area. Differently from previous reports, where a confined condensate or the presence of multiple, fragmented condensates have been associated with the presence of the disorder potential [6,7], the high spatial homogeneity of the present sample and the absence of potential defects in the region under study clearly indicate that we observe a purely self-induced localization.

It is interesting to note that, despite the small size of the localized condensate, its shape can be externally controlled by reshaping the pump beam. To prove this point, the horizontal and vertical elongations of the laser spot have been induced by cylindrical lenses in the optical excitation path (top row in Fig. 3). The ellipticity of the shape of the excitation spot is imprinted on the localized polariton condensate, as shown in the central row of Fig. 3 and in the magnified contour plot of the emission intensity in Figs. 3(e) and 3(f) (cross section profiles shown in Supplemental Material [18]). Conversely, the localization is absent when a top-hat laser spot profile is used (see Supplemental Material [18]), showing that a gradient of the potential landscape is needed. This suggests that localization occurs at the position of the highest exciton density, where the condensation threshold is first reached, and it is fed by a net flux of polaritons directed towards the localization point.

Numerical simulations.—The real-space collapse of a polariton condensate indicates the presence of a self-induced trapping mechanism capable of overcoming the intrinsic polariton-polariton repulsion. This requires an effective attractive interaction that cannot be explained in the conventional theoretical framework used for polaritons, that is a generalized Gross-Pitaevskii equation with positive interaction constants. We attribute this attraction to the polariton energy renormalization induced by the heat released during the condensation. Polariton thermalization to the ground state is assisted by the emission of the acoustic phonons which heat the crystal lattice and may locally change the lattice temperature by several degrees [21]. This leads to a local modification of the polariton dispersion and results in the formation of the trap at the position of the condensate density peak where the

temperature is maximal. This trap triggers the real-space collapse of the condensate and its shrinkage into a tight spot. The self-trapped state is further stabilized due to the stimulated scattering of reservoir excitons to the condensate.

To describe our experiments, we use the Ginzburg-Landau equation for the polariton order parameter Ψ coupled to the kinetic equation for the density n of incoherent polaritons (see Supplemental Material [18]). The effective attractive interaction is proportional to the rate of polariton relaxation from the reservoir to the ground state which is determined by the product of their densities, $|\Psi|^2 n$. Searching for the stationary solution in the case of a symmetric Gaussian pump, we reproduce the experimentally observed real-space condensate distribution, see Fig. 2 and Supplemental Material, Fig. S1.

In Fig. 4(a), the energy blueshift of the polariton condensate is measured for increasing pumping powers and compared to the results of simulations (above threshold). The formation of the polaronlike self-trapped state is accompanied by the change in the slope of the dependence of blueshift on the pump power visible at $P = P_{\mathrm{th}}$ in Fig. 4(a), with a slower increase above threshold. For excitation powers $P > P_{\mathrm{th}}$, the localization in real space corresponds to a delocalized emission in the reciprocal space (see Fig. 1), with the product of the standard deviations of the position and momentum distributions approaching the limit imposed by the Heisenberg uncertainty principle, $\Delta x \Delta k = 0.5$ [Fig. 4(b)]. This shows that the polaron self-trapping mechanism studied here results in the formation of the strongest possible localized polariton condensate with the widest possible distribution in k space. The range of k states available at the energy of the condensate is limited by the two bright spots visible in Fig. 1(e).

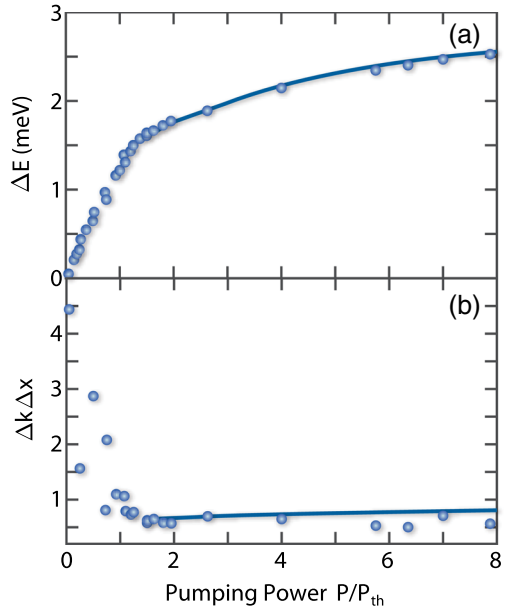

FIG. 4. (a) The measured (dots) and calculated (lines) blueshift of the condensate energy as a function of the pump power (FWHM of the laser spot is 20 μm). (b) The standard deviations Δx and Δk are obtained by fitting the PL intensity of the polariton condensate in real space and reciprocal space with a Gaussian function (see Supplemental Material [18]). Above threshold, the localized polariton condensate achieves the Heisenberg limit ($\Delta x \Delta k = 0.5$). The value of $\Delta x \Delta k$ as a function of power calculated numerically is shown by the blue line (above threshold).

In conclusion, the self-trapped stationary state of bosonic condensates of exciton polaritons can be referred to as a bosonic polaron phase. Indeed, the attractive interaction of polaritons is governed by their coupling with the crystal lattice that is a signature of a polaron. In contrast to conventional Pekar polarons [1] the dressing of a polariton condensate is produced by the local heating of the lattice rather than by its mechanical deformation. The number of polaritons contributing to the bosonic polaron is estimated as 2×10^3 [see Fig. 1(g)]. We estimate the local lattice temperature variation in the center of the polaron state as being of the order of 10 K (see Supplemental Material [18]). The strong dependence of the shape of a polaron state on the geometry of the pumping light beam offers an opportunity for efficient optical manipulation of polaron states that is crucial for their applications in polariton simulators.

Funding from the POLAFLOW ERC Starting Grant and the ERC project ElecOpteR Grant No. 780757 are acknowledged. The work of I. C. and A. K. is supported by Westlake University (Project No. 041020100118). A. K. also acknowledges the financial support from the Russian Foundation for Basic Research (RFBR Project No. 19-52-12032) and Deutsche Forschungsgemeinschaft (DFG) in the framework of International Collaborative Center TRR 160 and Saint-Petersburg State University for a research grant ID 40847559. The support from the Ministry of Science and Higher Education of the Russian Federation (state Project No. 16.5592.2017/6.7) is acknowledged by I. C. The Authors thank P. Cazzato for technical support.

[1] L. D. Landau and S. I. Pekar, J. Exp. Theor. Phys. **18**, 419 (1948).
[2] M. Koschorreck, D. Pertot, E. Vogt, B. Fröhlich, M. Feld, and M. Köhl, Nature (London) **485**, 619 (2012).
[3] T. Dietl and J. Spałek, Phys. Rev. Lett. **48**, 355 (1982).
[4] S. M. Ryabchenko and Yu. G. Semenov, Zh. Eksp. Teor. Fiz. **84**, 1419 (1983).
[5] J. Kasprzak, M. Richard, S. Kundermann, A. Baas, P. Jeambrun, J. M. J. Keeling, F. M. Marchetti, M. H. Szymańska, R. André, J. L. Staehli *et al.*, Nature (London) **443**, 409 (2006).
[6] J. Kasprzak, R. André, Le Si Dang, I. A. Shelykh, A. V. Kavokin, Y. G. Rubo, K. V. Kavokin, and G. Malpuech, Phys. Rev. B **75**, 045326 (2007).

[7] K. G. Lagoudakis, B. Pietka, M. Wouters, R. André, and B. Deveaud-Plédran, Phys. Rev. Lett. **105**, 120403 (2010).
[8] H. Ohadi, R. L. Gregory, T. Freegarde, Y. G. Rubo, A. V. Kavokin, N. G. Berloff, and P. G. Lagoudakis, Phys. Rev. X **6**, 031032 (2016).
[9] I. A. Shelykh, T. C. H. Liew, and A. V. Kavokin, Phys. Rev. B **80**, 201306(R) (2009).
[10] L. Dominici, M. Petrov, M. Matuszewski, D. Ballarini, M. De Giorgi, D. Colas, E. Cancellieri, S. B. Fernández, A. Bramati, G. Gigli *et al.*, Nat. Commun. **6**, 8993 (2015).
[11] P. G. Lagoudakis and N. G. Berloff, New J. Phys. **19**, 125008 (2017).
[12] N. G. Berloff, M. Silva, K. Kalinin, A. Askitopoulos, J. D. Töpfer, P. Cilibrizzi, W. Langbein, and P. G. Lagoudakis, Nat. Mater. **16**, 1120 (2017).
[13] I. Y. Chestnov, T. A. Khudaiberganov, A. P. Alodjants, and A. V. Kavokin, Phys. Rev. B **98**, 115302 (2018).
[14] D. Ballarini, D. Caputo, C. Sánchez Muñoz, M. De Giorgi, L. Dominici, M. H. Szymańska, K. West, L. N. Pfeiffer, G. Gigli, F. P. Laussy, and D. Sanvitto, Phys. Rev. Lett. **118**, 215301 (2017).
[15] Y. Sun, P. Wen, Y. Yoon, G. Liu, M. Steger, L. N. Pfeiffer, K. West, D. W. Snoke, and K. A. Nelson, Phys. Rev. Lett. **118**, 016602 (2017).
[16] D. Caputo, D. Ballarini, G. Dagvadorj, C. Sánchez Muñoz, M. De Giorgi, L. Dominici, K. West, L. N. Pfeiffer, G. Gigli, F. P. Laussy *et al.*, Nat. Mater. **17**, 145 (2018).
[17] M. Steger, C. Gautham, D. W. Snoke, L. Pfeiffer, and K. West, Optica **2**, 1 (2015).
[18] See Supplemental Material at http://link.aps.org/supplemental/10.1103/PhysRevLett.123.047401 for details on the experimental setup and numerical simulations, results of the excitation with a top-hat laser spot profile and with an elliptically shaped excitation spot.
[19] E. Wertz, L. Ferrier, D. D. Solnyshkov, R. Johne, D. Sanvitto, A. Lemaître, I. Sagnes, R. Grousson, A. V. Kavokin, P. Senellart *et al.*, Nat. Phys. **6**, 860 (2010).
[20] E. Kammann, T. C. H. Liew, H. Ohadi, P. Cilibrizzi, P. Tsotsis, Z. Hatzopoulos, P. G. Savvidis, A. V. Kavokin, and P. G. Lagoudakis, Phys. Rev. Lett. **109**, 036404 (2012).
[21] S. Klembt, E. Durupt, S. Datta, T. Klein, A. Baas, Y. Léger, C. Kruse, D. Hommel, A. Minguzzi, and M. Richard, Phys. Rev. Lett. **114**, 186403 (2015).